Heliyon 10 (2024) e29506

Contents lists available at ScienceDirect

Heliyon

journal homepage: www.cell.com/heliyon

Research article

A model for SARS-CoV-2 virus transmission on the upper deck of a passenger ship bound for a short trip

Zobair Ibn Awal [a,*], Md Rafsan Zani [a], Md Abu Sina Ibne Albaruni [b], Tawhidur Rahman [a], Md Shariful Islam [c]

[a] Department of Naval Architecture and Marine Engineering, Bangladesh University of Engineering and Technology (BUET), Dhaka, 1000, Bangladesh
[b] Department of Mechanical Engineering, Bangladesh University of Engineering and Technology (BUET), Dhaka, 1000, Bangladesh
[c] Department of Naval Architecture and Offshore Engineering, Bangabandhu Sheikh Mujibur Rahman Maritime University, Bangladesh (BSMRMU), Dhaka, 1216, Bangladesh

ARTICLE INFO

Keywords:
SARS-CoV-2 transmission
Public transport
Water transport
Passenger ship
Probabilistic modeling

ABSTRACT

Public transportation plays a critical role in meeting transportation demands, particularly in densely populated areas. The COVID-19 pandemic has highlighted the importance of public health measures, including the need to prevent the spread of the virus through public transport. The spreading of the virus on a passenger ship is studied using the Computational Fluid Dynamic (CFD) model and Monte Carlo simulation. A particular focus was the context of Bangladesh, a populous maritime nation in South Asia, where a significant proportion of the population utilizes passenger ships to meet transportation demands. In this regard, a turbulence model is used, which simulates the airflow pattern and determines the contamination zone. Parameters under investigation are voyage duration, number of passengers on board, social distance, the effect of surgical masks, and others. This study shows that the transmission rate of SARS-CoV-2 infection on public transport, such as passenger ships, is not necessarily directly proportional to voyage duration or the number of passengers onboard. This model has the potential to be applied in various other modes of transportation, including public buses and airplanes. Implementing this model may help to monitor and address potential health risks effectively in the public transport networks.

Nomenclature

F_D	Drag force (Newton)
g	Gravitational acceleration components (m/s^2)
k	Turbulent kinetic energy (J)
K	Fluid Thermal Conductivity (W/m K)
n	Number of particles
P	Pressure (Pa)
S	Source Term
t	Time (s)
T	Temperature (K)

(*continued on next page*)

* Corresponding author.
E-mail addresses: zobair@name.buet.ac.bd (Z.I. Awal), rafsanzani949@gmail.com (M.R. Zani), abusina.me@gmail.com (M.A.S.I. Albaruni), tawhidurrahman98@gmail.com (T. Rahman), sharif.naoe@gmail.com (M.S. Islam).

https://doi.org/10.1016/j.heliyon.2024.e29506
Received 4 September 2023; Received in revised form 4 March 2024; Accepted 9 April 2024
Available online 16 April 2024

(*continued*)

u, v, w	Velocity components (m/s)
V	Velocity vector (m/s)
x, y, z	Cartesian directions (m)
α	Thermal diffusivity (m^2/s)
ε	Dissipation rate of the turbulent energy
μ	Dynamic viscosity (m^2/s)
ρ	Density (kg/m^3)
d	Particle

1. Introduction

Public transport systems have been significantly impacted by the COVID-19 pandemic, which is caused by the highly contagious coronavirus. The virus is named Severe Acute Respiratory Syndrome Coronavirus-2 or SARS-COV-2 [1]. The first reported case of COVID-19 was in December 2019 in Wuhan, Hubei, China [2]. Person-to-person spreading of contagious pathogens mainly occurs because of human sneezing or coughing [3]. The droplets (size greater than 5 μm) and aerosols (size less than 5 μm) generated from the coughing and sneezing of an infected person contain the virus [4]. Human exhalation flows such as coughing, and sneezing can create

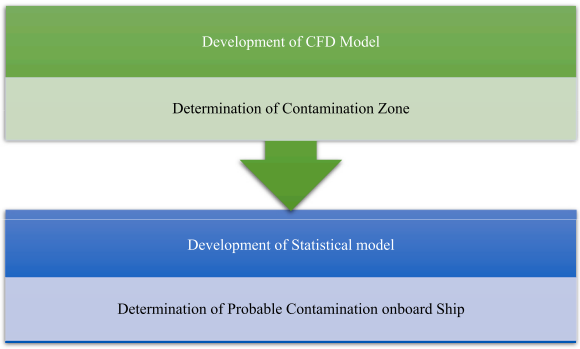

Fig. 1. Workflow of the study in terms of mathematical modeling.

Table 1
Boundary conditions.

Domain size	**3.8 m × 2.7 m × 2.9 m**
Height of the human body	1.83 m
Velocity inlet	0 m/s
Room temperature	300 K
Pressure	101.325 kPa

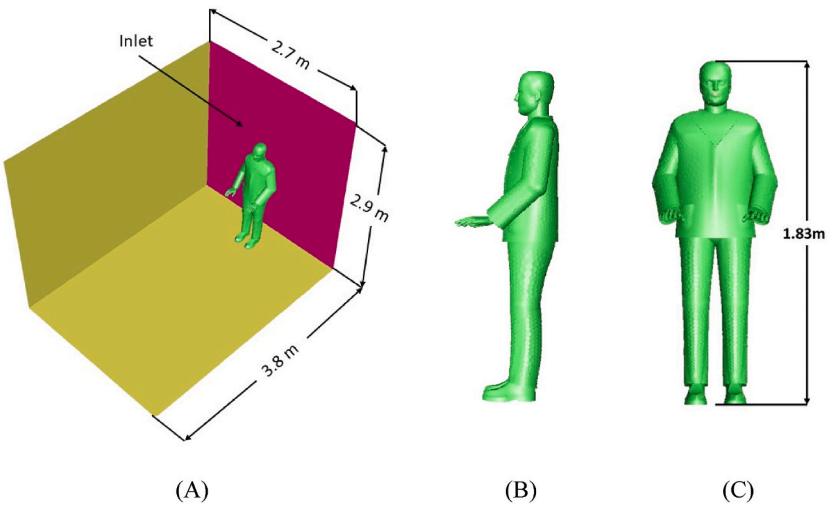

Fig. 2. (A) Domain used for simulation with dimension (B) side view of the human body and (C) front view of the human body used for simulation.

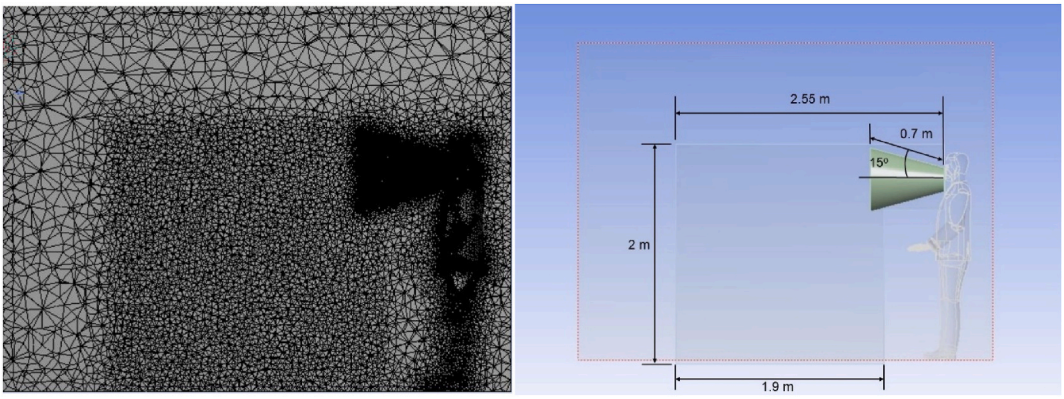

Fig. 3. (A) 2D view of mesh (B) 2D geometry of the mesh.

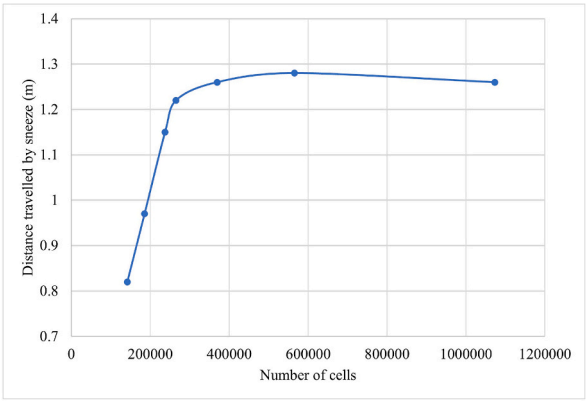

Fig. 4. Grid independence test.

Table 2
Principal particulars of the passenger's vessel.

Length (Over All)	84.91 m
Breadth	13.12 m
Depth	2.75 m
Draft (Loaded)	1.80 m
Dimension of Passenger Deck	35.5 m × 13.12 m

Fig. 5. A typical passenger ship in Bangladesh.

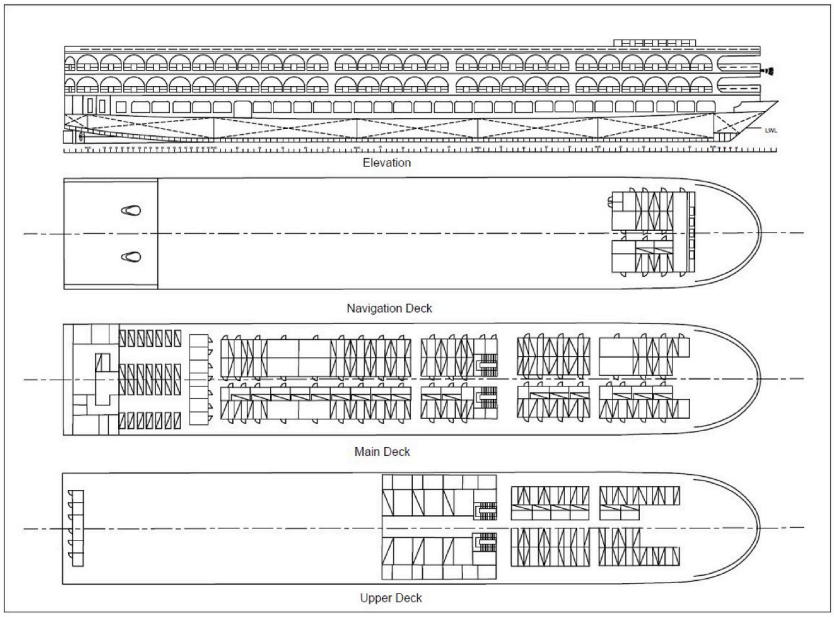

Fig. 6. General arrangement plan of the passenger's vessel.

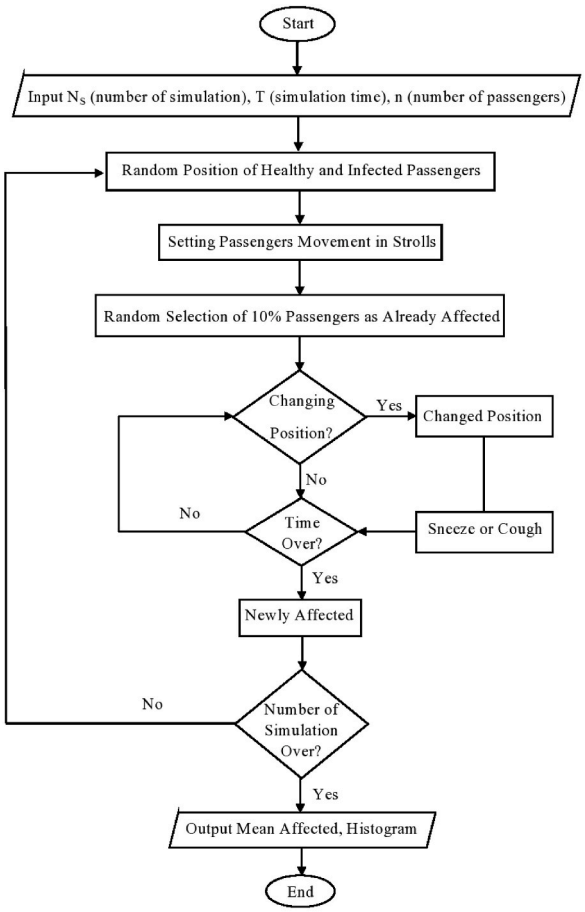

Fig. 7. Flow chart of the algorithm.

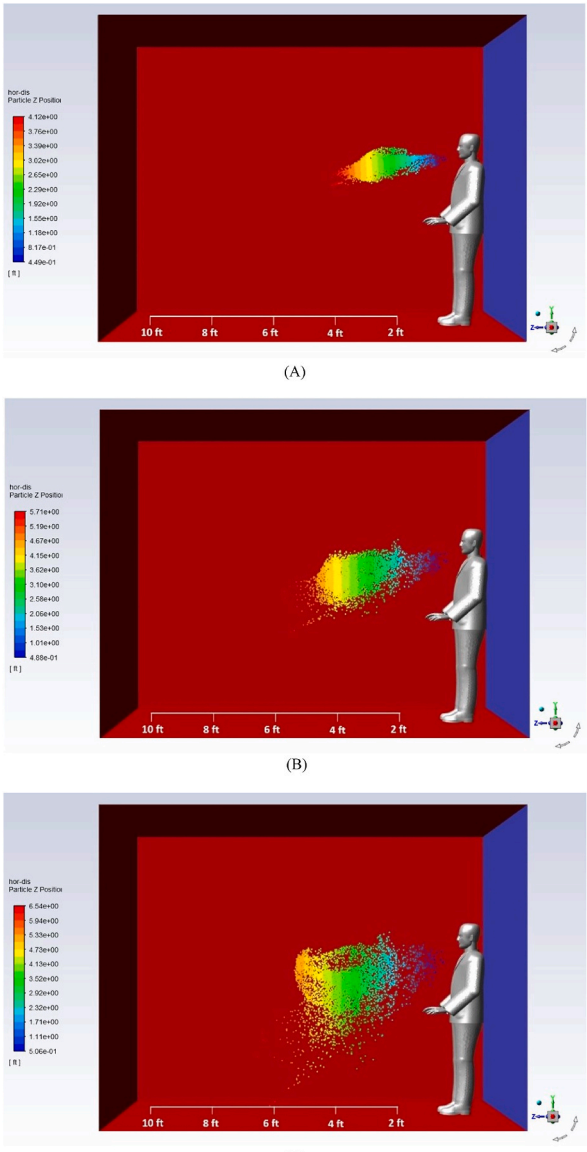

Fig. 8. Horizontal sneeze particle distribution at different time frames at: (A) 0.25 s; (B) 0.50 s; (C) 0.83 s.

Jet-like air flows [5], facilitating the spread of the virus from person to person. In addition to direct and indirect contact, the virus can spread through aerosol and droplet routes [6], posing a significant risk to passengers and crews in public transport. Comprehending and measuring the dissemination of the virus in public transportation networks is crucial in assessing the health impacts of different approaches and strategies. To achieve this, transportation and epidemiological models must be coupled to analyze contact graphs and spatial consequences [7]. This involves tracking individual passenger trajectories and using key performance indicators to assess the spread of the virus [8]. In addition, various climatic factors such as temperature, humidity, wind speed, and air quality are significantly associated with the transmission of the virus [9], highlighting the need for effective measures to prevent the spread of COVID-19 in public transport systems. Other factors such as population density, domestic movement, number of infected people, and solar radiation correlate with the infection rate [10].

Olmedo et al. [11] observed that the exhaled contaminants' exposure level depends on the air distribution system of a room, people's positions, activity level or height, exhalation direction, and other factors. A human sneeze generally lasts for just 0.3–0.7 s and the droplets exhaled at different times during the sneeze have the same distribution properties [12]. Guo et al. [6] examined the hospital wards of Wuhan, China, and showed how the virus was distributed in air, floor, and object surfaces in the hospital wards. Various measures come into practice to contain the infection rate, such as isolation, social distancing, quarantine, and community-wide containment [13]. The Centers for Disease Control (CDC) and World Health Organization (WHO) previously suggested maintaining a social distance of around 3–6 ft or 0.9–1.8 m [14]. Pendar and Páscoa [15] described the transmission mechanism

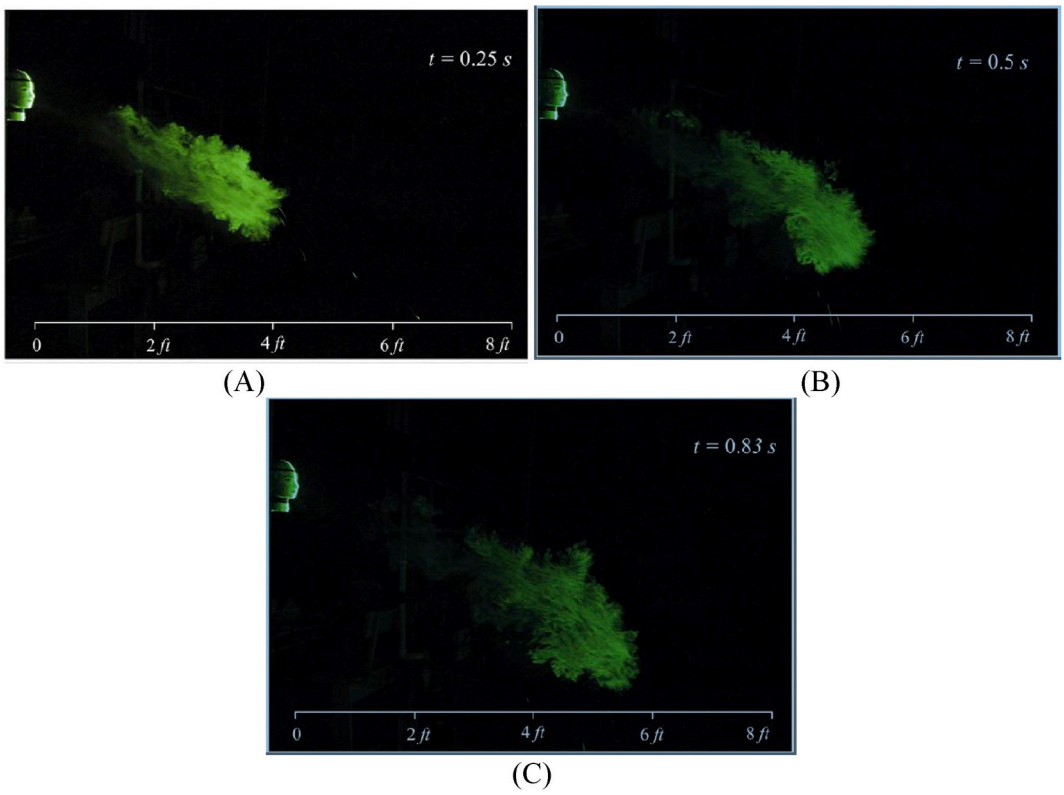

Fig. 9. Sneeze particle horizontal distribution at different time frames, experiment conducted by Arumuru et al. [17] (A) 0.25 s; (B) 0.50 s; (C) 0.83 s.

Table 3
Comparison between simulation and experimental results [17] of distance traveled by sneeze particles.

Time (s)	Computational Distance (ft)	Experimental Distance (ft)
0.25	4.1	4.1
0.5	5.1	5.1
0.83	5.4	5.6

of saliva droplets carried by vectors that can spread illness. The study proposed that the safe distance during sneezing must be at least 4 m. To understand the flow physics of the virus or the harmful agents, measures such as face masks, hand washing, and ventilation of the indoor environment are typically suggested nowadays [16]. A three-layer homemade mask and using the elbow or hand to prevent droplet leakage even after wearing a mask are also strongly recommended [17].

Over the years, several research works focused on simulating human coughing and sneezing. Villafruela et al. [18] developed a Computational Fluid Dynamics (CFD) model for the flow of human exhalation. Similarly, Busco et al. [19] also developed a CFD simulation model of a human sneeze. The studies suggest that a sneeze could influence a zone of 4 m in the downstream direction, 2 m in the horizontal direction, and 2 m in the lateral movement. Bhattacharyya et al. [20] showed that air conditioning machines mixed with aerosol sanitizer could effectively mitigate the effects of the COVID-19 virus in an isolation room.

According to Dbouk and Drikakis [21], the saliva droplets generated from coughing do not travel more than 1 m when the surrounding air is still. Moreover, when the person is wearing a surgical mask, the particle travel distance assumed is 0.5 m [22].

Hassan and Megahed [23] used a transient 3D CFD model to revisit the designs of urban space elements, considering the potential risks of viral transmission. They proposed nine models of public seating arrangement in urban places. They provided a better public seating option amid the ongoing pandemic. Alrebi et al. [24] also examined the emergency department design at a university hospital. Their investigation provided a better understanding of airflow patterns in emergency units. They also recommended using partitions or doors to separate the high-risk areas in emergency departments accordingly. Moreover, a detailed study of the distribution of harmful droplets in a classroom equipped with and without partitions has been conducted [25]. This study demonstrated that seat partitions for individuals could reduce the infection rate to a certain extent. Moreover, Bertone et al. [26] and Luo et al. [27] conducted a transmission risk assessment in public buses of SARS-COV-2 viruses. In the works of Bertone et al. [26], two types of buses were selected, one is the type of bus that commutes in urban areas and the other type is the long-distance bus. The authors concluded that a bus in an

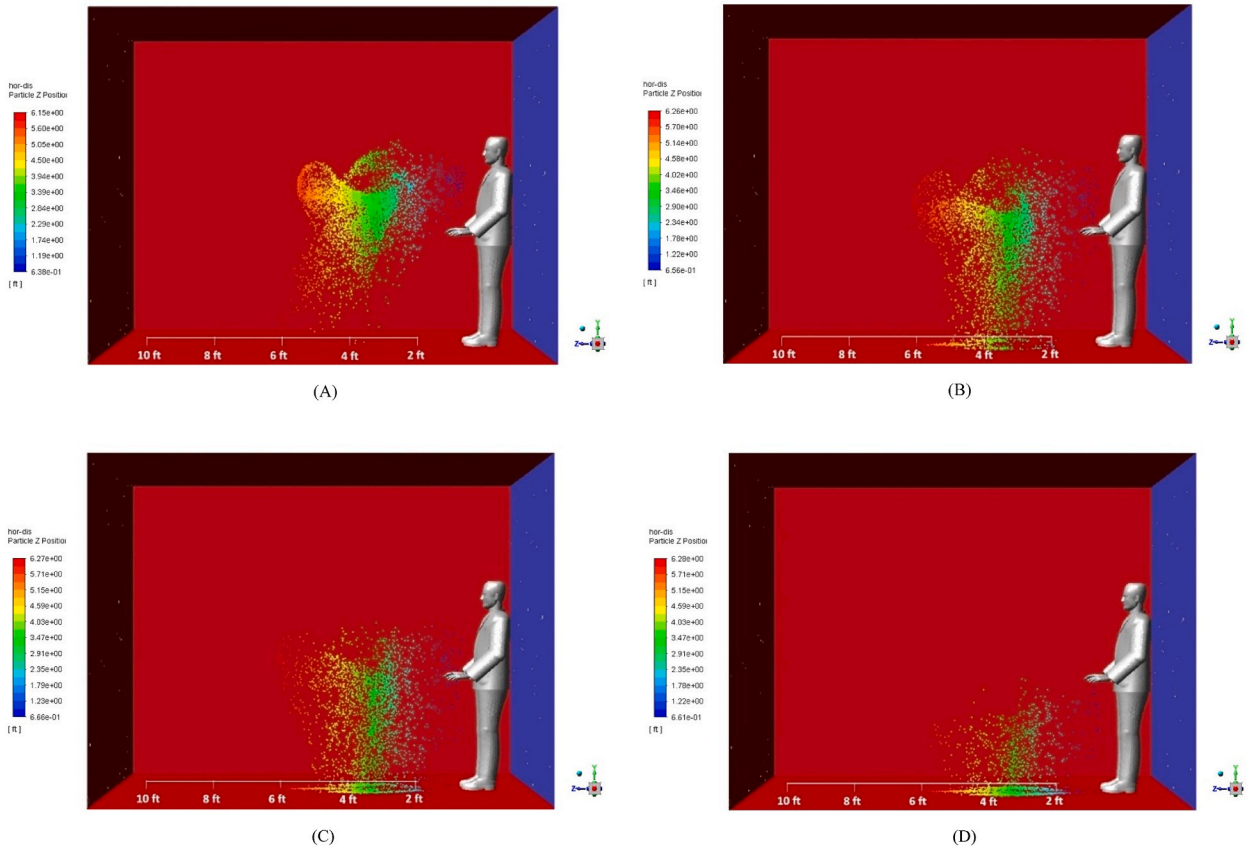

Fig. 10. Sneeze particle distribution at: (A) 1 s; (B) 2 s; (C) 3 s; (D) 5 s.

Table 4
Case studies considered for this research.

Case No.	People wearing masks	Social distance (m)
1	No	0.25
2	Yes	0.25
3	No	1.0
4	Yes	1.0
5	No	1.25
6	Yes	1.25

urban area would be at a higher transmission risk when fully occupied than long-distance buses. In closed spaces like engine rooms, heat stress should be considered while modeling for virus transmission. Palella et al. [28] worked on the management of heat stresses in the closed spaces of ships.

The literature review suggests that in the past, significant developments have taken place in the discipline of fluid and particle flow analysis with a particular focus on viral transmissions. Nevertheless, the safety of the water transportation system in Bangladesh has caught international attention quite frequently [29,30] and public health issues such as virus transmission within public water transport have not been addressed in detail in the recent past. Therefore, this research focuses on COVID-19 virus transmission on the deck of a passenger ship operating in one of the most populous South Asian countries, Bangladesh, where most of the population uses passenger ships for commutes.

2. Mathematical model formulation

This section discusses the fundamentals of mathematical modeling developed and utilized in this research. Fig. 1 shows the workflow and the outcomes of the study. This study shows the development of a numerical model of the flow dynamics of the COVID-19 virus, which uses a turbulence model to find out the distance traveled by the droplets. The droplets released from coughing and sneezing of COVID affected persons can carry harmful viruses and other harmful agents such as SARS-COV-2. This is especially

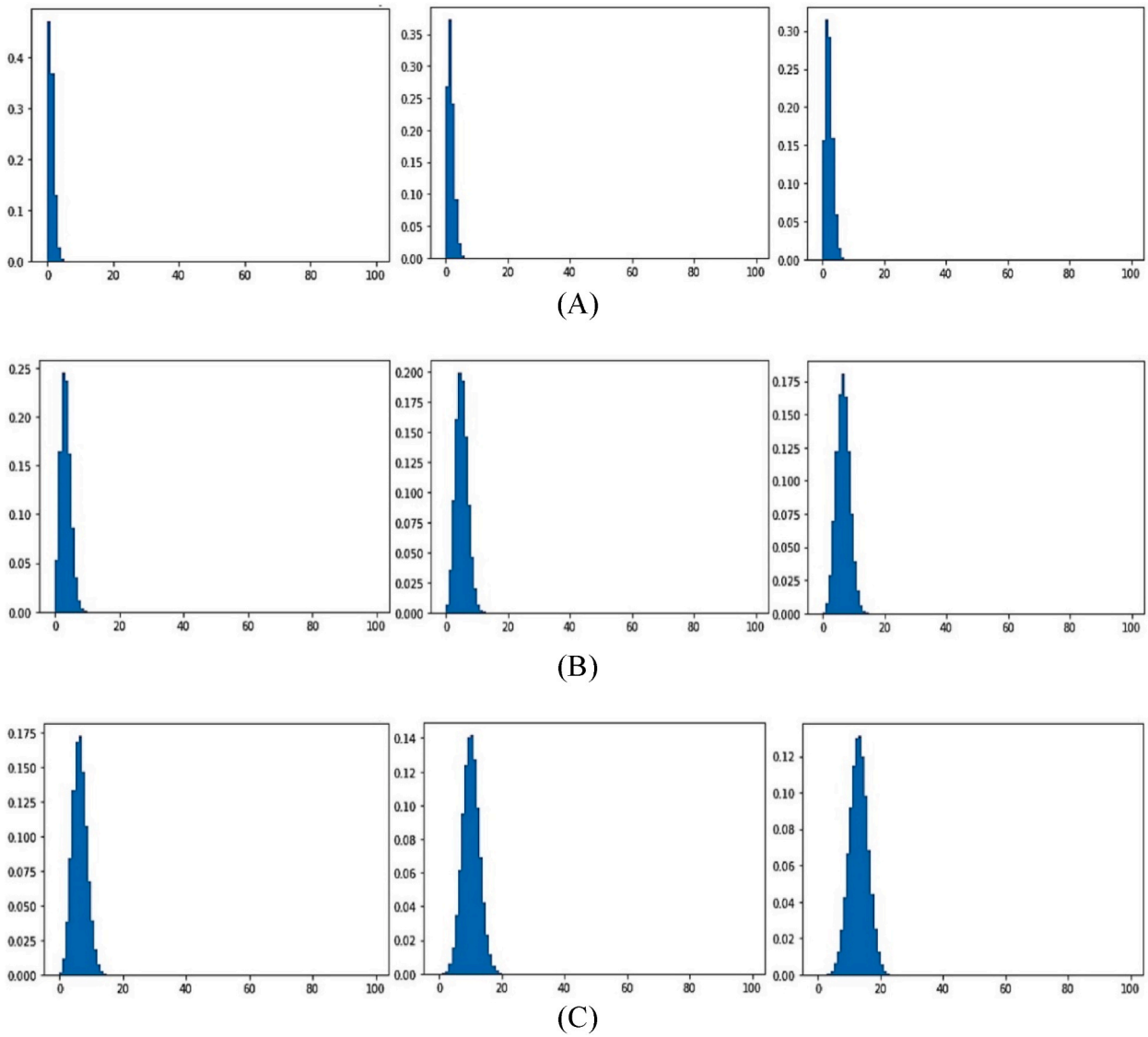

Fig. 11. Probability distribution histogram (Case 1) of newly infected people for duration of 1 h, 2 h, 3 h (from left to right) for (A) 10 people (B) 20 people (C) 30 people (D) 50 people (E) 75 people (F) 100 people.

concerning in public transport systems where passengers are close to one another, and the distance traveled by the sneeze or cough particle determines the zone of probable contamination. Therefore, this paper focuses on developing a statistical model that calculates the probability of newly affected people, which is vital for controlling the spread of COVID-19 in public transport.

2.1. Theoretical background of the CFD model

Governing equations of airflow expressed in the general equations for conservation of mass, momentum and energy are as follows:

$$\frac{\partial \rho}{\partial t} + \nabla . \left(\rho \overrightarrow{V} \right) = 0 \tag{1}$$

$$\rho \left(\frac{\partial \overrightarrow{V}}{\partial t} + \overrightarrow{V} . \nabla \overrightarrow{V} \right) = - \nabla \mathrm{P} + \mu \nabla^2 \overrightarrow{V} + \rho \overrightarrow{g} \tag{2}$$

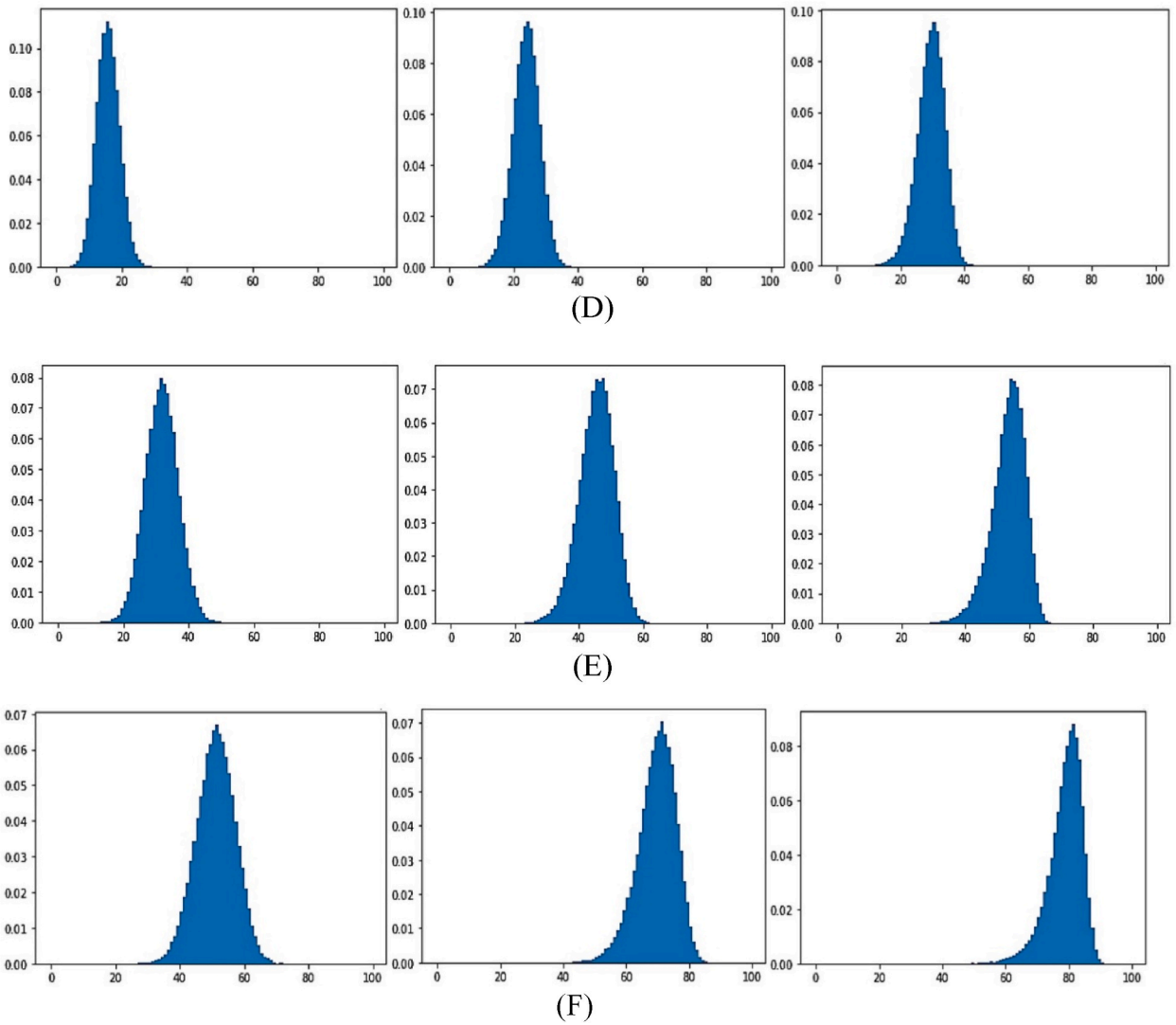

Fig. 11. (*continued*).

$$\rho\frac{\partial T}{\partial t}+\rho\vec{\nabla}.\left(\mathrm{T}\vec{V}\right)=\nabla.\left(\frac{K}{C_p}\nabla T\right)+S_T \tag{3}$$

For the turbulent flow analysis, the *RNG* $k-\varepsilon$ turbulence model is famous for simulating the air droplets mixture having recirculating flows. The transport equations for turbulent kinetic energy (k) and dissipation rate (ε) are given as:

$$\frac{\partial}{\partial t}(\rho k)+\frac{\partial}{\partial x_i}(\rho k u_i)=\frac{\partial}{\partial x_j}\left[\alpha_k\ \mu_{eff}\ \frac{\partial k}{\partial x_j}\right]+G_k+S_k-\rho\varepsilon \tag{4}$$

$$\frac{\partial}{\partial t}(\rho\varepsilon)+\frac{\partial}{\partial x_i}(\rho\varepsilon u_i)=\frac{\partial}{\partial x_j}\left[\alpha_\varepsilon\ \mu_{eff}\ \frac{\partial\varepsilon}{\partial x_j}\right]+C_{1\varepsilon}\frac{\varepsilon}{k}G_k+S_\varepsilon-\left(C_{2\varepsilon}\rho\frac{\varepsilon^2}{k}+R_\varepsilon\right) \tag{5}$$

Here, G_k is the generated turbulent kinetic energy due to mean velocity gradients. S_k and S_ε are user-defined source terms. R_ε is the source term from renormalization. α_k and α_ε are adequate inverse Prandtl numbers corresponding to the turbulent kinetic energy and its dissipation. μ_{eff} is the turbulent viscosity. Moreover, $C_{1\varepsilon}$ and $C_{2\varepsilon}$ are model constants.

2.2. Discrete phase

There are a few assumptions in the discrete phase modelling similar to the work of Bahramian et al. [31]. The assumptions are:

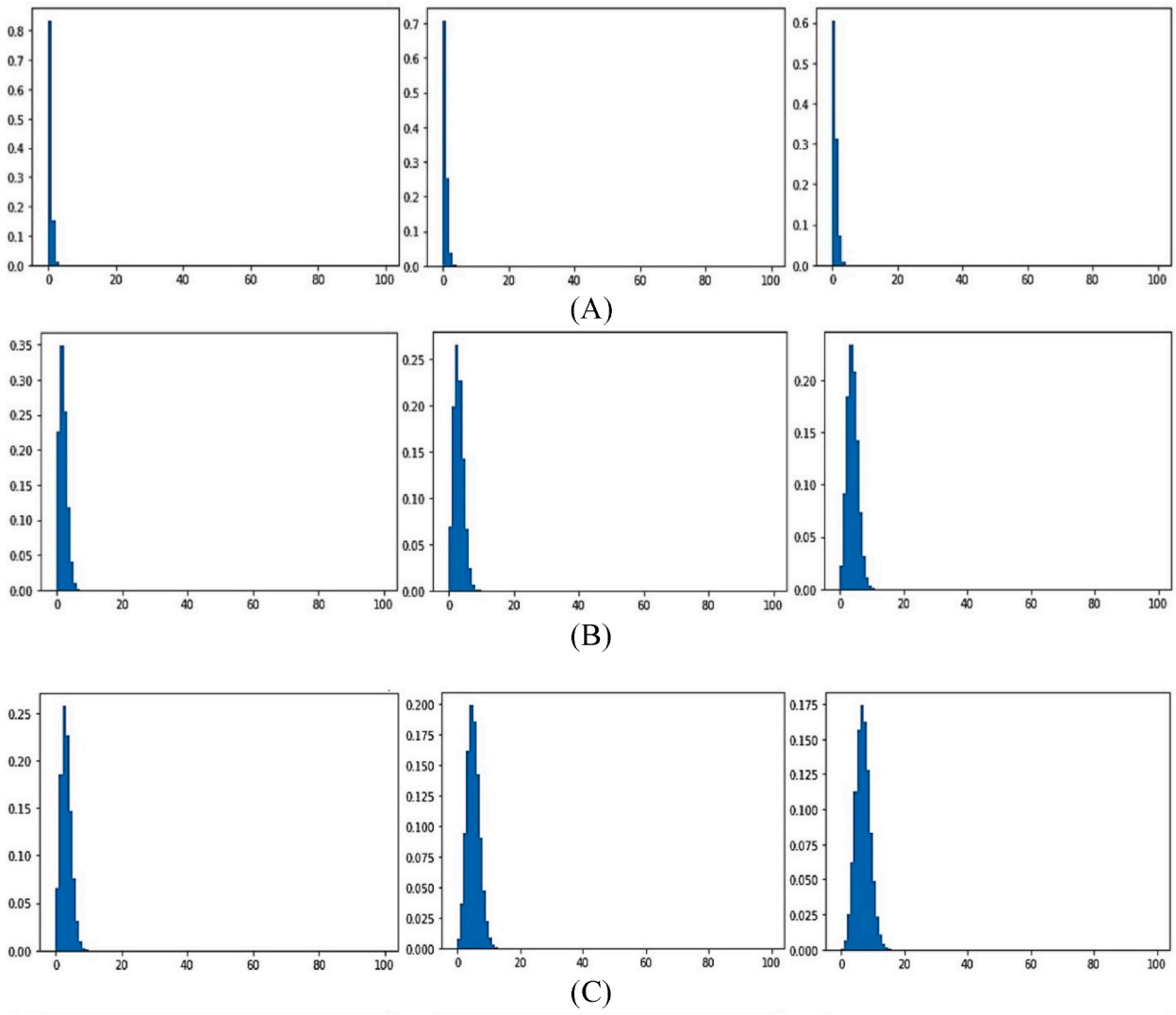

Fig. 12. Probability distribution histogram (Case 2) of newly infected people for duration of 1 h, 2 h, 3 h (from left to right) for (A) 10 people (B) 20 people (C) 30 people (D) 50 people (E) 75 people (F) 100 people.

1. The sneeze airflow temperature remained constant (300 K) throughout the simulations.
2. Only one sneeze was modeled.
3. All droplets were spherical in shape.
4. Only the droplet particles emitted from the human mouth during sneeze was considered.
5. The effect of the humidity field generated due to evaporation of the dispersed sneeze particles, was not considered.
6. The effect of non-volatile compounds, such as salts and lipids, was ignored.

An air-water mixture is used for the particle trajectory analysis. Using Newton's second law in the Lagrangian framework, the trajectories of pathogen-carrying droplets are evaluated [32,33]. The equation of motion is given as:

$$\frac{d\vec{V}_d}{dt} = F_D\left(\vec{V} - \vec{V}_d\right) + \frac{\vec{g}(\rho_d - \rho)}{\rho_d} \tag{6}$$

Here, F_D is the Drag force which is given by:

$$F_D = \frac{3\mu C_D R_e}{4{D_d}^2 \rho_d} \tag{7}$$

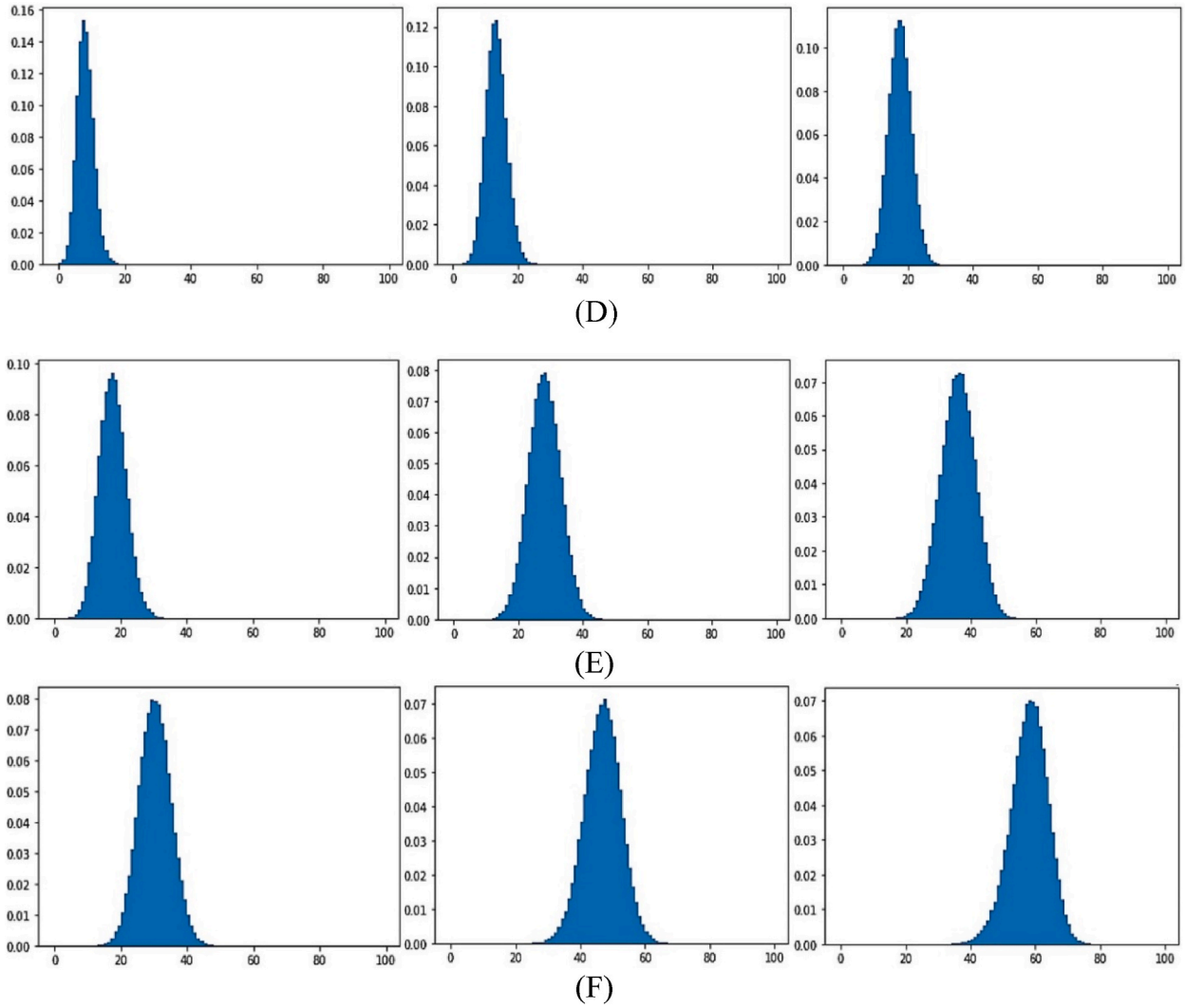

Fig. 12. (*continued*).

Where, μ is the molecular viscosity, D_d is the diameter of the particle and C_D is the drag-coefficient of the particle [34].

The equation of mass flow rate is:

$$\dot{m} = \frac{\left(\frac{4}{3}\pi r^3\right) \times \rho_d \times n}{t} \tag{8}$$

where n is the number and ρ_d is the density of particles.

2.3. CFD setup

The CFD simulation is performed using ANSYS Fluent package. The geometry construction and meshing are done on the ANSYS package. Polyhedral-type mesh modeling is used in this work. The coupling solver is used to capture the discrete phase model.

For the boundary conditions (shown in Table 1), the domain is a cuboid room where the human model remains, and the room's dimension is 3.8 m × 2.7 m × 2.9 m, as shown in Fig. 2A. Fig. 2B and C shows the side and front views of the human body. The height of the human body is 1.83 m (6 ft). The surface of the cuboid behind the human body is taken as an inlet where the velocity is 0 m/s. The top, front, left and right surfaces of the cuboid room are altogether considered as pressure outlet. The room temperature is 300 K at one atmospheric pressure (101.325 kPa).

The study considers the sneezing time of 0.2 s and the average sneezing velocity of 40 m/s [17]. The total mass flow rate of a sneeze is 0.02 kg/s. Droplets of various sizes have a minimum diameter of 5 μm and a maximum diameter of 80 μm [12]. The mean droplet

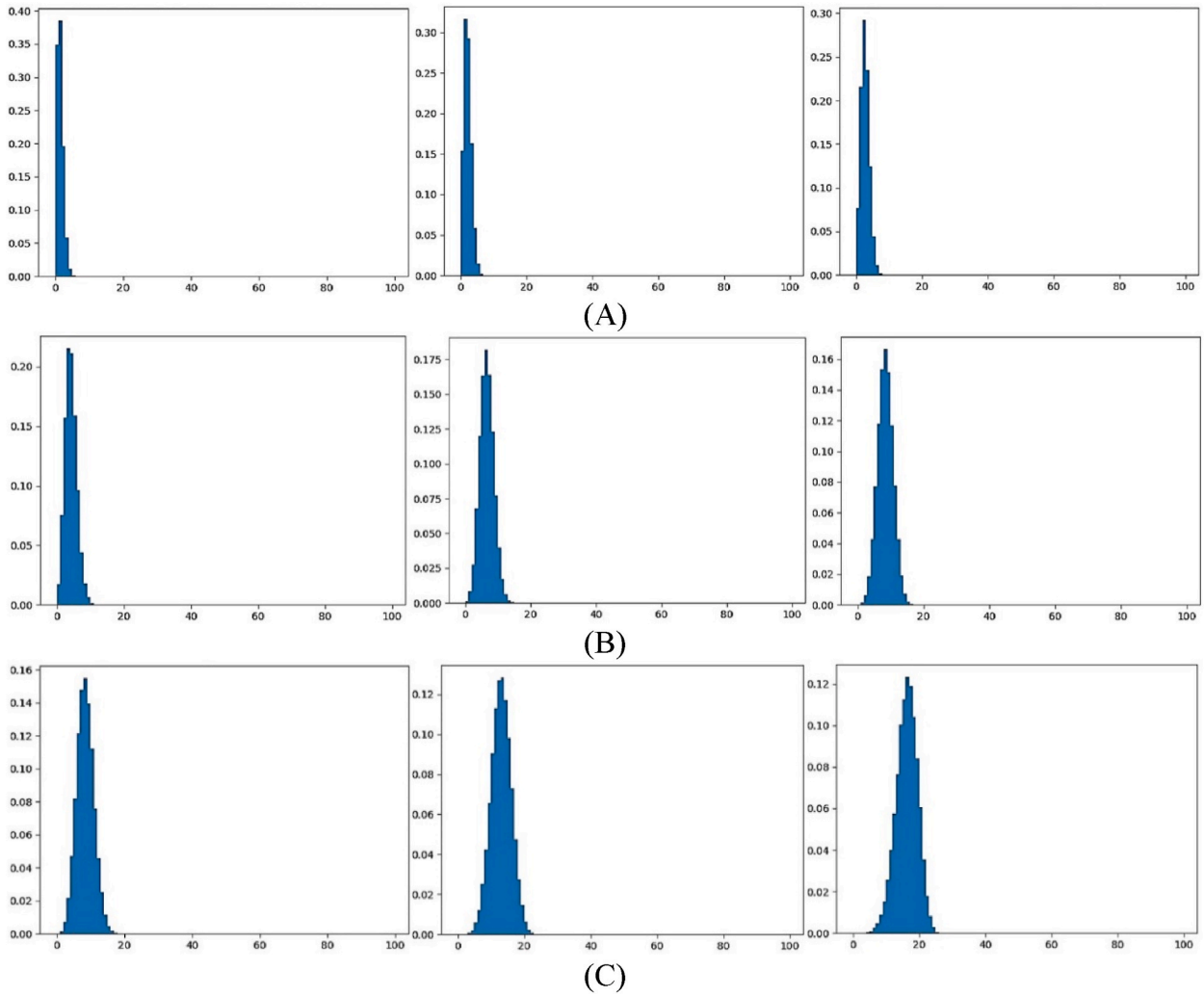

Fig. 13. Probability distribution histogram (Case 3) of newly infected people for duration of 1 h, 2 h, 3 h (from left to right) for (A) 10 people (B) 20 people (C) 30 people (D) 50 people (E) 75 people (F) 100 people.

diameter is 14 μm. For size distribution of droplets, the Rosin-Rammler distribution approach was adopted. Droplet loading fraction was 0.7 at the nostrils and the turbulence intensity from the nostrils of the human body is assumed as 5 %. These values of the droplet diameters were incorporated in the discrete phase modeling.

For unsteady CFD analysis, the time step was 0.01 s and the inner iteration number was 15. The total iteration number was 7500 for 5 s of simulation. These variables were optimized through iteration for faster convergence while keeping a lower computational expense. The convergence criteria for the CFD scheme were met when all residuals in the turbulence model equations were less than 10^{-4}.

The following are assumptions for this simulation:

1. Temperature variations are negligible.
2. Human cough emits air and droplet mixture.
3. There is no slip condition between phases.
4. Virus-infected droplets are particles.
5. The surrounding air is still.

2.4. Grid independence test

The number of cells used for simulation can significantly affect the accuracy of the result. Hence, a grid independence test is needed

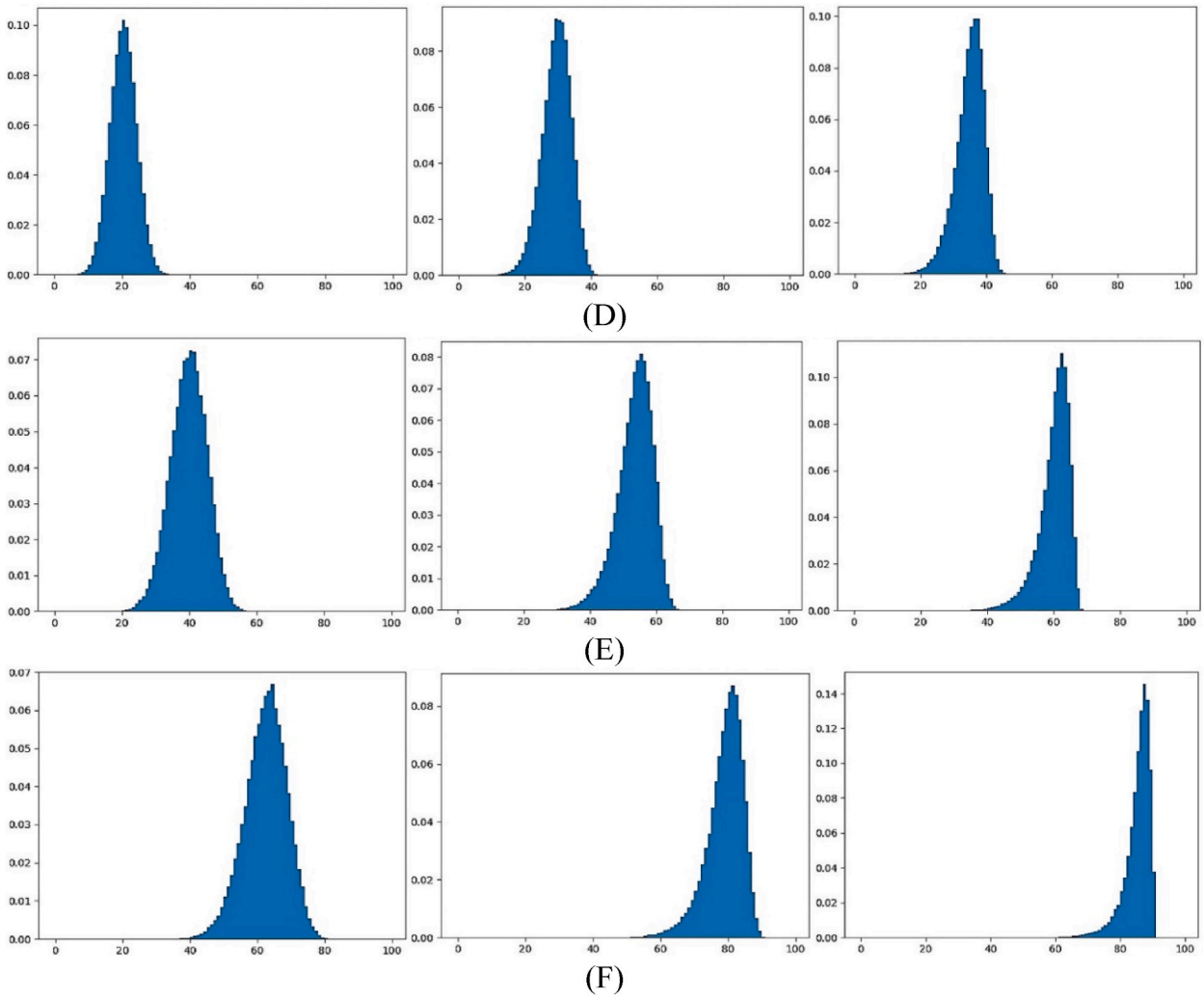

Fig. 13. (*continued*).

to ensure that the simulation results are independent of the grid size. In this study, a tetrahedral mesh was created using ANSYS-fluent. The sneezing velocity is constant throughout the grid independence test. Fig. 3A shows the meshed model. The mesh is denser and finer in proximity to the mouth so that the dispersed air-droplet mixture can be captured with enhanced precision. The cone angle of 30°, determined through iteration, was constructed from the mouth of the human-body for mesh refinement. Fig. 3B shows the dimensional geometry of the body.

For the independence test, seven different grid-size models are considered to determine the best size at which the distance becomes insignificant to the computation of the distance traveled by the exhaled sneeze and cough particles. The number of cells ranges from 142015 (coarse) to 1073003 (the finest). Fig. 4 reveals that after the model of 369780 cells, the relative deviation in the computed distance for cell number is insignificant. To validate the simulated results with the experimental results of Arumuru et al. [17], the elapsed time for the grid independency was 0.83 s. It shows that a grid sizing with 369780 cells is sufficient for modeling the exhalation of particles from the passenger in the room.

2.5. Formulation of probabilistic model

A probabilistic model is constructed to study the spreading of the virus onboard a passenger ship. At first, the particulars of the passenger's vessel are discussed. The ship is built of steel, typically found in the inland waterways of South Asian countries (such as Bangladesh). The vessel is 85 m long and can carry as many as 800 people. Typical speed varies due to traffic and weather; however, the maximum speed may reach nearly 12 knots. The principal particulars are given in Table 2. A picture of a typical passenger ship and its general arrangement plan is shown in Figs. 5 and 6, respectively.

For the probabilistic analysis, this study considers several parameters, such as the number of sneezes per hour per passenger, the percentage of the infected passenger, dynamics of passenger movements, and the number of passengers with and without masks.

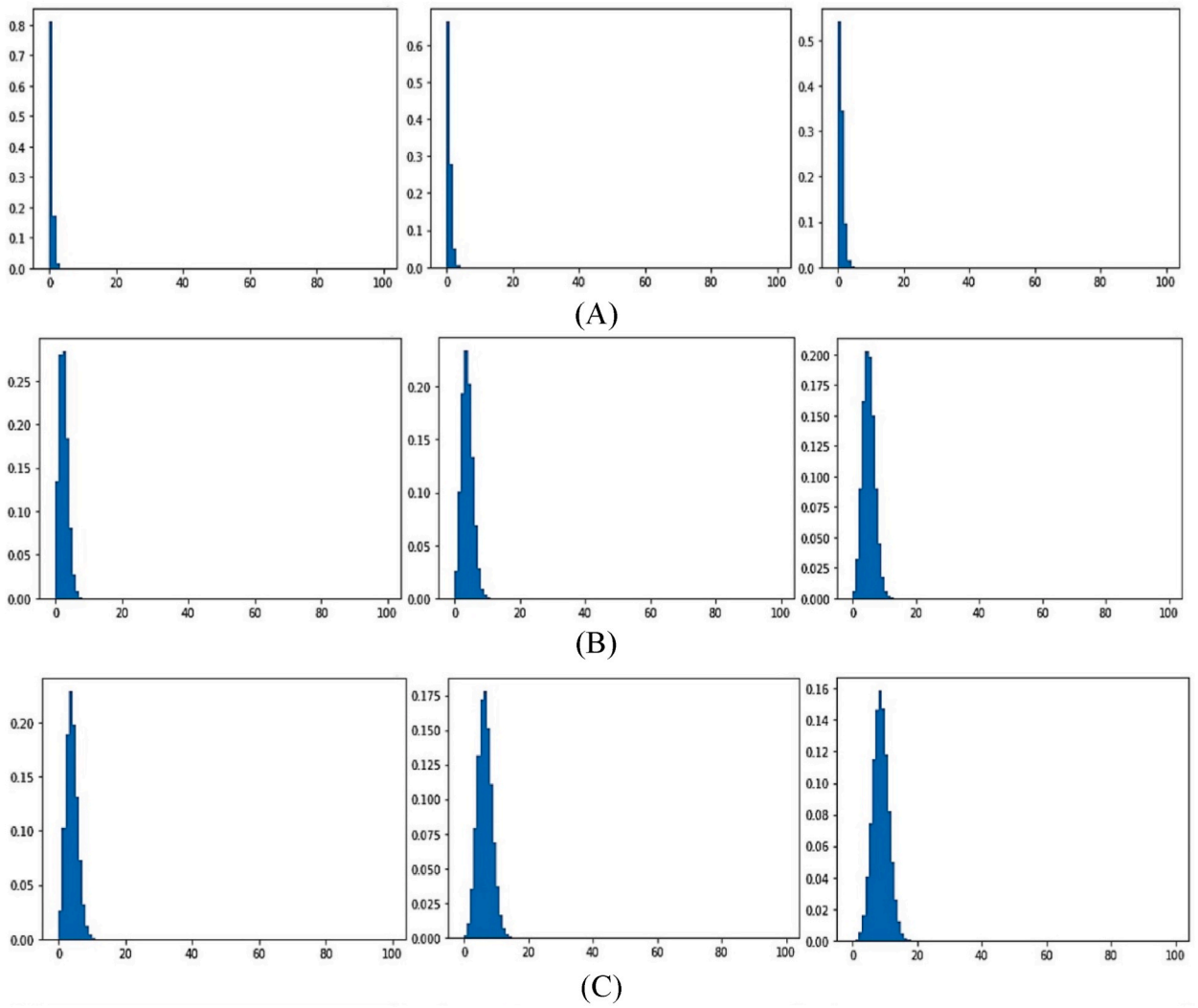

Fig. 14. Probability distribution histogram (Case 4) of newly infected people for duration of 1 h, 2 h, 3 h (from left to right) for (A) 10 people (B) 20 people (C) 30 people (D) 50 people (E) 75 people (F) 100 people.

Gwaltney et al. [35] observed that the maximum number of times a cold patient sneezed in a day was 17. However, this study assumes that a patient sneezes 24 times in one day (once every hour). The assumption continues as 10 % of the population (taken randomly) traveling on the deck are infected by the COVID-19 virus and may infect other people. Although there are enough seating arrangements, people frequently walk around the deck. However, it is assumed that each of them randomly roams 20 % of the voyage time. Each stroll is limited to 3 min in the stretch while the passenger walks up to 2 m per minute, 0.033 m/s. Finally, it is assumed that 50 % of the passengers use surgical masks. The mask's efficacy is 75 % [36]. An algorithm is shown in Fig. 7, following which the mask reduces the probability of getting affected by the specific conditions, as mentioned above, by 75 %.

In the statistical model, proximity plays a crucial role in COVID-19 transmission dynamics. If an infected individual sneezes and a healthy person is within a 2 m radius at that moment, the healthy person is deemed susceptible to infection. The CFD simulation shows that after around 5 s the droplets descend at a certain distance where the effects caused by those droplets become negligible. So, we assumed that the horizontal distance covered by the droplets in 5 s as the risk zone. The radius of the risk zone has been used in the probabilistic model. The model also considers coughing, which reduces the distance of potential exposure to 1 m. These findings underscore the nuanced factors influencing the risk of COVID-19 transmission and contribute to a more detailed understanding in the spread of the virus.

The CFD results determined the maximum distance sneeze particles travel. In the probabilistic model, this distance became the radius of a circle, representing the COVID-19 risk zone. Anyone inside this circle is potentially exposed to the virus. This statistical model helps us see areas where there might be a risk and better understand how the virus can spread in different places.

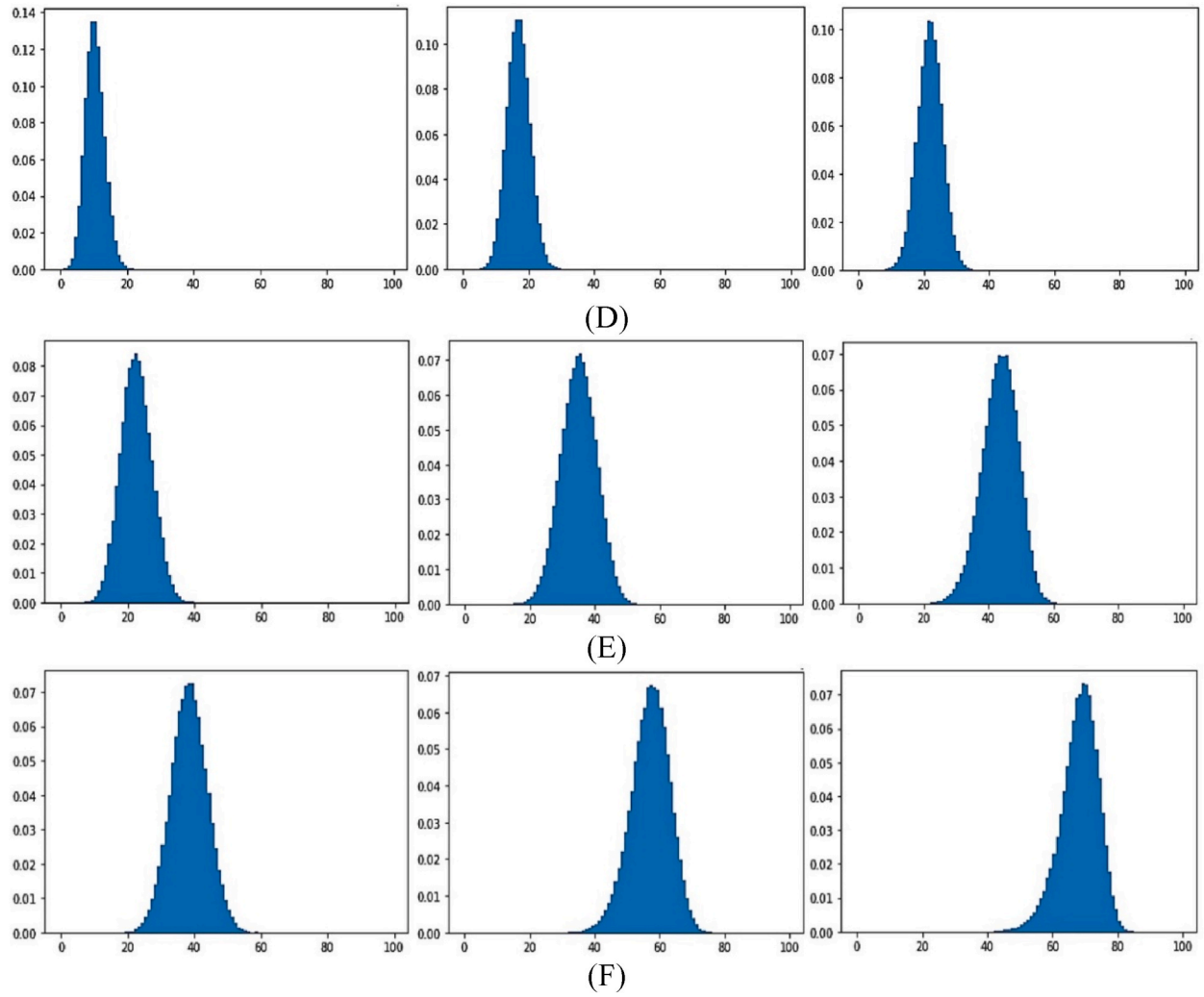

Fig. 14. (*continued*).

3. Validation of theoretical CFD model

The validation of the CFD simulation is conducted in this section. Arumuru et al. [17] studied the sneeze distribution experimentally, where the horizontal distribution of sneeze particles was recorded in different time steps. In this research, similar time steps are taken to study the distribution of particles in the horizontal direction (shown in Fig. 8). The experimental study by Arumuru et al. [17] is shown in Fig. 9.

The results shown in Fig. 8 agree with the experimental study Arumuru et al. [17] conducted. There are slight deviations as some of the particles in the simulation traveled farther. This anomaly is due to a few particles traveling farther from the sneeze cloud. If only the cloud were considered, the computational results would be close to the experimental results. Table 3 compares the computational and experimental results for time frames of 0.25 s, 0.50 s, and 0.83 s.

4. Results and discussion

The spread of sneeze particles for up to 5 s is computed using the CFD simulation software. The farthest distance the particles cover is 6.26 ft (1.9 m), and the particles eventually get dropped on the floor as time passes. At around 5 s, the direction of motion of most of the particles is downwards. The whole sneeze distribution at different time durations is illustrated in Fig. 10.

Six different case studies have been considered in this research. Table 4 shows a list of case studies. The cases differ by the parameters of social distance and the status of wearing masks. The probabilistic computation is applied, and the number of possible newly affected people is determined. This calculation is repeated 1,00,000 times to get probabilistic results, and the probability of the number of newly affected people is calculated. After that, histograms are plotted to depict the probability distribution for various cases.

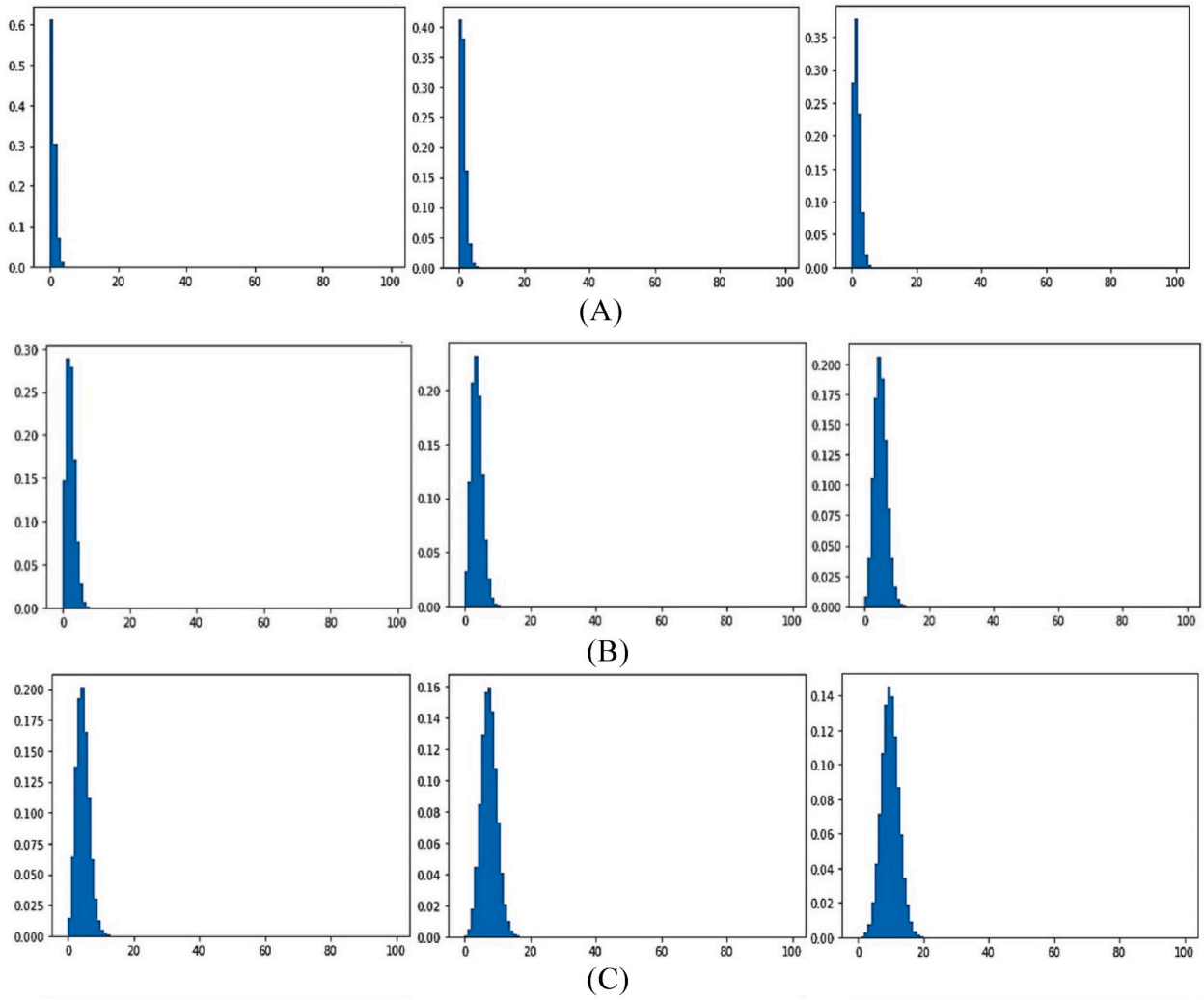

Fig. 15. Probability distribution histogram (Case 5) of newly infected people for duration of 1 h, 2 h, 3 h (from left to right) for (A) 10 people (B) 20 people (C) 30 people (D) 50 people (E) 75 people (F) 100 people.

Case 1. Case 1 comprises unmasked people, and the social distance maintained among them is 0.25 m. The probability distribution of newly affected passengers are shown in Fig. 11 for 10, 20, 30, 50, 75, and 100 people for different voyage times. From Fig. 11, it is observed that the histograms of probability distribution get to the maximum for a certain number of people and shows the highest possible number of people that can get infected, with the lowest probability, and the number of newly affected people with the highest chance. For 1–3 h, when 20 people are considered, at most 10 to 22 people are newly affected, and 4 to 8 freshly affected people have the highest probability. When 50 people are considered, at most, 28 to 42 people are newly affected, and 19 to 35 freshly affected people have the highest chance. When 100 people are considered, at most 70 to 90 people are newly affected, and 58 to 80 freshly affected people have the highest likelihood of getting infected by the virus.

Case 2. In Case 2, 50 % of the population is masked, and the social distance remains unchanged (0.25 m). The probability distribution is shown in Fig. 12 for 10, 20, 30, 50, 75, and 100 people for different voyage times. The histogram plots follow the same trend as Case 1. For 1–3 h, when 20 people are considered, at most 8 to 12 people are newly affected, and 2 to 7 freshly affected people have the highest probability. When 50 people are considered, 18 to 30 people are newly affected, and 9 to 20 freshly affected people have the highest chance. When 100 people are considered, at most 48 to 78 people are newly affected, and 35 to 65 freshly affected people have the highest probability of getting infected by the virus.

Case 3. All of them are unmasked, and the social distance maintains 1 m. The probability distribution is shown in Fig. 13 for 10, 20, 30, 50, 75, and 100 people for different voyage times. When 20 people are considered in the duration ranging from 1 to 3 h, at most 10 to 18 people are newly affected, and 3 to 5 freshly affected people have the highest probability. When 50 people are considered for the

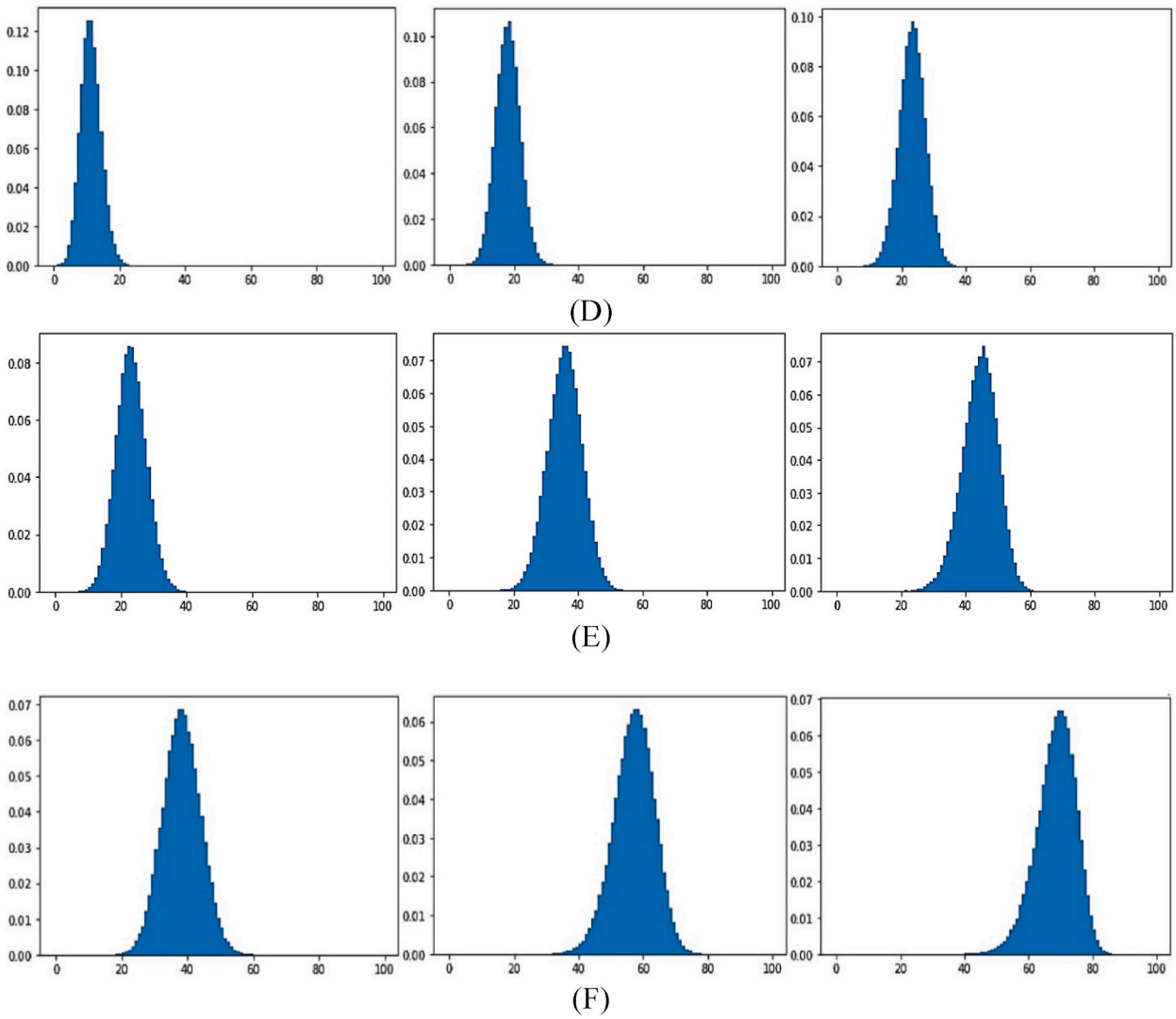

Fig. 15. (*continued*).

same duration range, at most, 32 to 46 people are newly affected, and 18 to 33 freshly affected people have the highest probability. When 100 people are considered, 80 to 90 people are newly affected, and 62 to 88 freshly affected people are most likely to get infected by the virus.

Case 4. 50 % are masked, and the social distance is maintained to be 1 m. The probability distribution is shown in Fig. 14 for 10, 20, 30, 50, 75, and 100 people for different voyage times. For duration ranging from 1 to 3 h, when 20 people are considered, at most 8 to 16 people are newly affected, and 2 to 6 freshly affected people have the highest probability. When 50 people are considered for the same duration range, at most, 20 to 36 people are newly affected, and 12 to 24 freshly affected people have the highest probability. When 100 people are considered, 58 to 82 people are newly affected, and 40 to 75 freshly affected people are most likely to get infected by the virus.

Case 5. They are unmasked, and the social distance is maintained at 1.25 m. The probability distribution is shown in Fig. 15 for 10, 20, 30, 50, 75, and 100 people for different voyage times. When 20 people are considered in the duration ranging from 1 to 3 h, at most, 7 to 12 people are newly affected, and 3 to 5 freshly affected people have the highest probability of getting infected. When 50 people are considered for the same duration range, at most, 22 to 38 people are newly affected, and 12 to 25 freshly affected people have the highest probability of getting infected. When 100 people are considered, at most 58 to 83 people are newly affected, and 40 to 74 freshly affected people have the highest probability of getting infected by the virus.

Case 6. 50 % are masked, and the social distance is maintained at 1.25 m. The probability distribution is shown in Fig. 16 for 10, 20, 30, 50, 75, and 100 people for different voyage times. For 1–3 h, when 20 people are considered, at most 6 to 10 people are newly

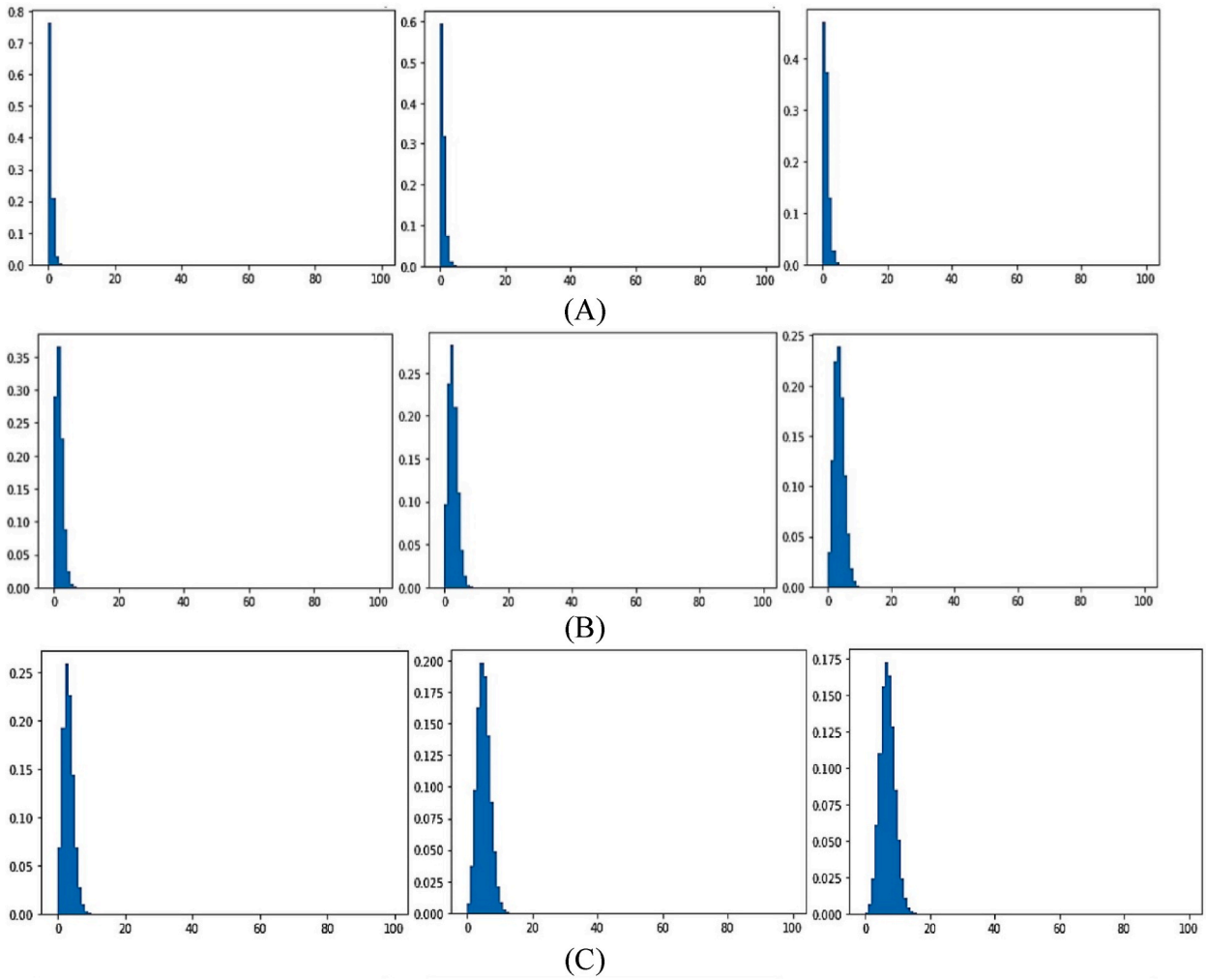

Fig. 16. Probability distribution histogram (Case 6) of newly infected people for duration of 1 h, 2 h, 3 h (from left to right) for (A) 10 people (B) 20 people (C) 30 people (D) 50 people (E) 75 people (F) 100 people.

affected, and 1 to 3 freshly affected people have the highest probability. When 50 people are considered for the same duration range, at most, 17 to 28 people are newly affected, and 8 to 18 freshly affected people have the highest probability. When 100 people are considered, 41 to 72 people are newly affected, and 26 to 58 freshly affected people have the highest likelihood of getting infected by the virus.

After completing the probability distribution histogram, the mean rate of newly affected people is calculated. The graph is plotted where the abscissa is time in hours, and the ordinate is the mean of newly affected persons in percentage, as shown in Fig. 17. In all the cases, six graphs have been generated based on the number of people on the deck. For all the graphs in Fig. 17, when only ten people are considered, a non-linear graph is recorded with a slight curve at the beginning where the value in the ordinate increases at a decreasing rate. This graph has the lowest varying gradient. When 100 people are considered, the graph's line is the steepest in the beginning. It follows the trend of varying angles where the percentage of newly affected people increases at a decreasing rate over time. The rest of the graphs between 10 and 100 people have the same properties but vary in ordinates. As the number of people on the deck increases, the initial slope becomes steeper, and the infection rate increases. Fig. 17 shows that the difference in infection rate is significantly higher between 30 and 50 people in all cases. Therefore, it can be deduced that the infection rate increases significantly when 50 people are considered to present on the deck.

On the other hand, wearing masks reduces the infection rate, as is seen in Fig. 17B, D, and 17F. The infection rate is lower than for those not wearing masks, as shown in Fig. 17A, C, and 17E. However, although the social distance was supposed to reduce the infection rate, Fig. 17C and D shows a higher infection rate than Fig. 17A and B. The reason for this anomaly is the random distribution. As the distance increases, more people will likely get covered by sneezing or coughing. It is because the initially affected people spread pathogenic particles all over the deck, unlike the simulation in 0.25 m (Fig. 17A and B), where they might not have spread pathogens

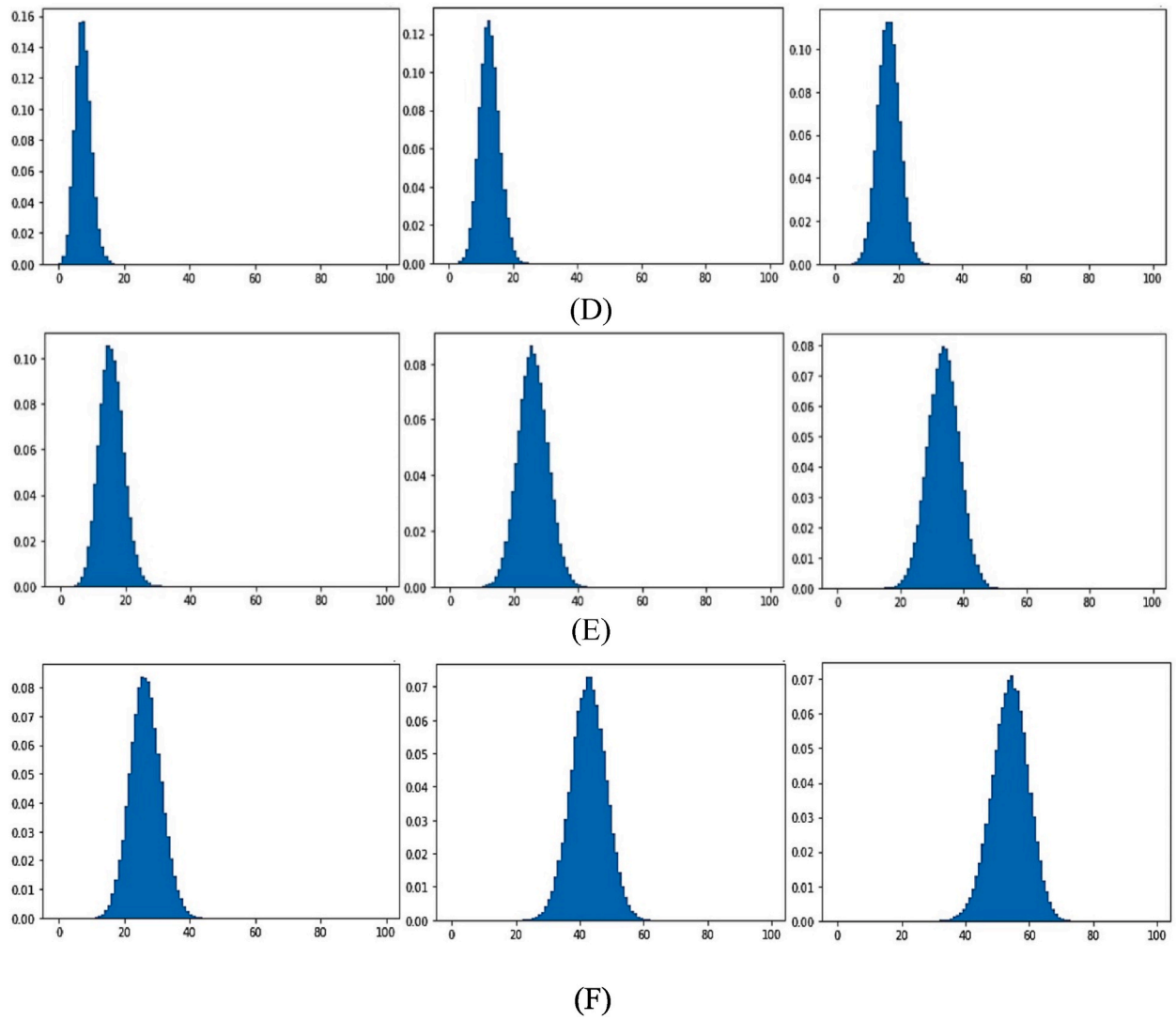

Fig. 16. (*continued*).

like these cases (Fig. 17C and D).

As the distance gets even more extensive in Fig. 17E and F, the infection rate reduces to the other cases since the space in these cases is larger than the cough spreading range but not the sneezing range.

Wearing a mask always reduces the infection rate, and case 6 shows the lowest infection rate of all cases, as shown in Fig. 17F. Therefore, from the graphs, it can be concluded that the infection rate differs by 11–23 % from the comparison of masked and unmasked cases of each maintained social distance. Governing equations of conservation in the case of incompressible steady airflow are expressed in the general equations for conservation of mass, momentum, and energy as follows:

5. Conclusion

This research presents a new approach to determining how the COVID-19 virus spreads on an upper deck of a passenger ship. A numerical simulation is conducted to determine the transmission of sneeze and cough particles on board the passenger ship. In addition, a probabilistic model is developed for computing new infections on the upper deck of the passenger ship bound for short trips of up to 3 h. The combined model evaluates six cases with varying populations, where social distance and wearing masks played a crucial role. Based on the analysis, the following conclusions may be drawn:

i. The graph shows that as the voyage time doubles, the mean infection rate increases but does not get doubled. The mean infection rate is not directly proportional to time. Still, the infection increases at a decreasing rate and eventually reaches a saturation point with a high infection rate in all cases as time increases.

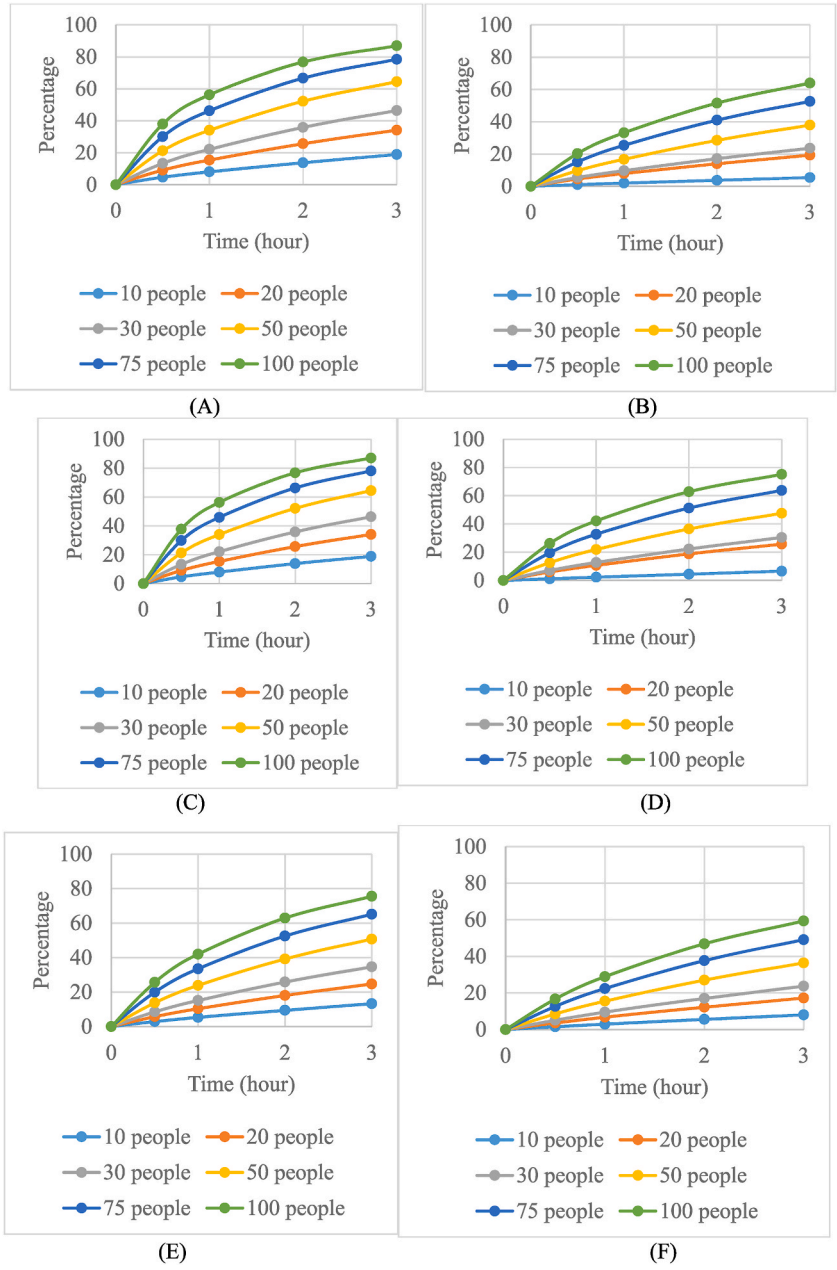

Fig. 17. Mean newly infected in percentage vs time graph for: (A) Case 1 (B) Case 2 (C) Case 3 (D) Case 4 (E) Case 5 (F) Case 6.

ii. It is seen that even with 1.25 m of social distance, there is a significant increase in mean infection rate even though the cough particles cannot travel this far. The highest traverse of sneeze particles is about 1.9 m, found from CFD results. Therefore, maintaining a social distance more than the highest traverse of sneeze particles would be safe.

iii. When social distance is varied between 0.25 m and 1.25 m, the change in infection rate remains within 12 %. On the other hand, the infection rate decreases significantly when half of the passengers are equipped with surgical masks. That means wearing a mask plays a more vital role in suppressing the infection rate than maintaining social distance up to 2 m.

iv. In cases 1 and 3, the virus is transmitted via human cough and sneeze particles. Cough droplets cannot reach other passengers in case 5 (social distance = 1.25 m). There is still a substantial increase in infection rate at the 3rd hour, but it is less than the infection rates in cases 1 and 3. So, it is visible that sneeze particles are more responsible for spreading the infection than cough particles.

v. 1 m social distance contributes more spreading of infection than a social distance of 0.25 m. However, as the distance increases, the spreading gets reduced again. Therefore, wearing a mask and maintaining proper social distance is essential to reduce infection.

More detailed numerical and statistical work is recommended to analyze sneeze and cough particles on public transports, such as passenger ships, by constructing models in all marine vessels' decks, cabins, stairways, and galleys. Extensive studies could be conducted by comparing infection rates among the ship's decks, and a probable red zone could be found based on passenger distribution. Moreover, the numerical study could introduce wind speed and humidity to get a more precise value of the particles traversed from a passenger's mouth. By incorporating these factors, more accurate results can be obtained, leading to a deeper understanding of the scenario of particle transmission in public transport.

Data availability statement

The authors agreed and stated that the data would be provided upon request.

CRediT authorship contribution statement

Zobair Ibn Awal: Writing – review & editing, Supervision, Project administration, Methodology, Investigation, Conceptualization. **Md Rafsan Zani:** Writing – original draft, Visualization, Validation, Software, Data curation. **Md Abu Sina Ibne Albaruni:** Software, Data curation, Validation, Visualization, Writing – original draft. **Tawhidur Rahman:** Writing – original draft, Data curation, Software, Validation, Visualization. **Md Shariful Islam:** Visualization, Validation, Software, Data curation, Writing – original draft.

Declaration of competing interest

The authors declare that they have no known competing financial interests or personal relationships that could have appeared to influence the work reported in this paper.

Acknowledgement

The authors would like to thank Basic Research Grant, Bangladesh University of Engineering and Technology (BUET), Dhaka 1000, Bangladesh for necessary funding support to conduct the research.

References

[1] A.E. Gorbalenya, S.C. Baker, R.S. Baric, R.J. de Groot, C. Drosten, A.A. Gulyaeva, B.L. Haagmans, C. Lauber, A.M. Leontovich, B.W. Neuman, D. Penzar, S. Perlman, L.L.M. Poon, D.V. Samborskiy, I.A. Sidorov, I. Sola, J. Ziebuhr, The species Severe acute respiratory syndrome-related coronavirus: classifying 2019-nCoV and naming it SARS-CoV-2, Nat. Microbiol. 5 (2020) 536–544, https://doi.org/10.1038/s41564-020-0695-z.

[2] N. Zhu, D. Zhang, W. Wang, X. Li, B. Yang, J. Song, X. Zhao, B. Huang, W. Shi, R. Lu, P. Niu, F. Zhan, X. Ma, D. Wang, W. Xu, G. Wu, G.F. Gao, W. Tan, A novel coronavirus from patients with Pneumonia in China, 2019, N. Engl. J. Med. 382 (2020) 727–733, https://doi.org/10.1056/nejmoa2001017.

[3] S. Seepana, A.C.K. Lai, Experimental and numerical investigation of interpersonal exposure of sneezing in a full-scale chamber, Aerosol. Sci. Technol. 46 (2012) 485–493, https://doi.org/10.1080/02786826.2011.640365.

[4] R. Zhang, Y. Li, A.L. Zhang, Y. Wang, M.J. Molina, Identifying airborne transmission as the dominant route for the spread of COVID-19, Proc. Natl. Acad. Sci. U. S.A. 117 (2020) 14857–14863, https://doi.org/10.1073/pnas.2009637117.

[5] J.W. Tang, A.D. Nicolle, C.A. Klettner, J. Pantelic, L. Wang, A. Bin Suhaimi, A.Y.L. Tan, G.W.X. Ong, R. Su, C. Sekhar, D.D.W. Cheong, K.W. Tham, Airflow dynamics of human jets: sneezing and breathing - potential sources of infectious aerosols, PLoS One 8 (2013) 1–7, https://doi.org/10.1371/journal.pone.0059970.

[6] Z.D. Guo, Z.Y. Wang, S.F. Zhang, X. Li, L. Li, C. Li, Y. Cui, R. Bin Fu, Y.Z. Dong, X.Y. Chi, M.Y. Zhang, K. Liu, K. Liu, C. Cao, B. Liu, K. Zhang, Y.W. Gao, B. Lu, W. Chen, Aerosol and surface distribution of Severe acute respiratory syndrome coronavirus 2 in hospital wards, Wuhan, China, 2020, Emerg. Infect. Dis. 26 (2020) 1586–1591, https://doi.org/10.3201/eid2607.200885.

[7] V. Colizza, M. Barthélemy, A. Barrat, A. Vespignani, Epidemic modeling in complex realities, Comptes Rendus Biol. 330 (2007) 364–374, https://doi.org/10.1016/j.crvi.2007.02.014.

[8] A. Tirachini, O. Cats, COVID-19 and public transportation: current assessment, prospects, and research needs, J. Publ. Transport. 22 (2020) 1–34, https://doi.org/10.5038/2375-0901.22.1.1.

[9] M.F. Bashir, B. Ma, Bilal, B. Komal, M.A. Bashir, D. Tan, M. Bashir, Correlation between climate indicators and COVID-19 pandemic in New York, USA, Sci. Total Environ. (2020) 728, https://doi.org/10.1016/j.scitotenv.2020.138835.

[10] M. Ahmadi, A. Sharifi, S. Dorosti, S. Jafarzadeh Ghoushchi, N. Ghanbari, Investigation of effective climatology parameters on COVID-19 outbreak in Iran, Sci. Total Environ. 729 (2020) 138705, https://doi.org/10.1016/j.scitotenv.2020.138705.

[11] I. Olmedo, P.V. Nielsen, M. Ruiz de Adana, R.L. Jensen, P. Grzelecki, Distribution of exhaled contaminants and personal exposure in a room using three different air distribution strategies, Indoor Air 22 (2012) 64–76, https://doi.org/10.1111/j.1600-0668.2011.00736.x.

[12] Z.Y. Han, W.G. Weng, Q.Y. Huang, Characterizations of Particle Size Distribution of the Droplets Exhaled by Sneeze, vol. 10, Journal of the Royal Society Interface, 2013, https://doi.org/10.1098/rsif.2013.0560.

[13] A. Wilder-Smith, D. Freedman, Isolation, quarantine, social distancing and community containment: pivotal role for old- style public health measures in the novel coronavirus (2019-nCoV) outbreak, J. Trav. Med. 27 (2020) 2–4, 10.1093/JTM/TAAA020.

[14] How to Protect Yourself and Others | CDC, (n.d.). https://www.cdc.gov/coronavirus/2019-ncov/prevent-getting-sick/prevention.html (accessed January 18, 2023).

[15] M.R. Pendar, J.C. Páscoa, Numerical modeling of the distribution of virus carrying saliva droplets during sneeze and cough, Phys. Fluids 32 (2020), https://doi.org/10.1063/5.0018432.

[16] R. Mittal, R. Ni, J.H. Seo, The flow physics of COVID-19, J. Fluid Mech. 894 (2020), 10.1017/jfm.2020.330.

[17] V. Arumuru, J. Pasa, S.S. Samantaray, Experimental visualization of sneezing and efficacy of face masks and shields, Phys. Fluids 32 (2020), https://doi.org/10.1063/5.0030101.
[18] J.M. Villafruela, I. Olmedo, M. Ruiz de Adana, C. Méndez, P.V. Nielsen, CFD analysis of the human exhalation flow using different boundary conditions and ventilation strategies, Build. Environ. 62 (2013) 191–200, https://doi.org/10.1016/j.buildenv.2013.01.022.
[19] G. Busco, S.R. Yang, J. Seo, Y.A. Hassan, Sneezing and asymptomatic virus transmission, Phys. Fluids 32 (2020), https://doi.org/10.1063/5.0019090.
[20] S. Bhattacharyya, K. Dey, A.R. Paul, R. Biswas, A novel CFD analysis to minimize the spread of COVID-19 virus in hospital isolation room, Chaos, Solit. Fractals 139 (2020), https://doi.org/10.1016/j.chaos.2020.110294.
[21] T. Dbouk, D. Drikakis, On coughing and airborne droplet transmission to humans, Phys. Fluids 32 (2020), https://doi.org/10.1063/5.0011960.
[22] P.P. Simha, P. Simha, M. Rao, Universal trends in human cough airflows at large distances Universal trends in human cough airflows at large distances, Phys. Fluids 32 (2020), https://doi.org/10.1063/5.0021666.
[23] A.M. Hassan, N.A. Megahed, COVID-19 and urban spaces: a new integrated CFD approach for public health opportunities, Build. Environ. (2021) 204, https://doi.org/10.1016/j.buildenv.2021.108131.
[24] O. Fawwaz, B. Obeidat, I. Atef, E.F. Darwish, A. Amhamed, Airflow dynamics in an emergency department : a CFD simulation study to analyse COVID-19 dispersion, Alex. Eng. J. 61 (2021), https://doi.org/10.1016/j.aej.2021.08.062.
[25] M. Mirzaie, E. Lakzian, A. Khan, M.E. Warkiani, O. Mahian, G. Ahmadi, COVID-19 spread in a classroom equipped with partition – a CFD approach, J. Hazard Mater. 420 (2021), https://doi.org/10.1016/j.jhazmat.2021.126587.
[26] M. Bertone, A. Mikszewski, L. Stabile, G. Riccio, G. Cortellessa, F.R. d'Ambrosio, V. Papa, L. Morawska, G. Buonanno, Assessment of SARS-COV-2 airborne infection transmission risk in public buses, Geosci. Front. 13 (6) (2022) 101398, https://doi.org/10.1016/j.gsf.2022.101398.
[27] K. Luo, Z. Lei, Z. Hai, S. Xiao, J. Rui, H. Yang, X. Jing, H. Wang, Z. Xie, P. Luo, W. Li, Q. Li, H. Tan, Z. Xu, Y. Yang, S. Hu, T. Chen, Transmission of SARS-COV-2 in public transportation vehicles: a case study in Hunan Province, China, Open Forum Infect. Dis. 7 (10) (2020), https://doi.org/10.1093/ofid/ofaa430.
[28] B.I. Palella, F. Quaranta, G. Riccio, On the management and prevention of heat stress for crews onboard ships, Ocean Eng. 112 (2016) 277–286, https://doi.org/10.1016/j.oceaneng.2015.12.030.
[29] M.J. Mia, M.I. Uddin, Z.I. Awal, A. Abdullah, An era of inland water transport accidents and casualties: the case of a low-income country, J. Int. Marit. Saf., Environ. Aff. Shipp. 5 (2021) 32–39, https://doi.org/10.1080/25725084.2021.1919432.
[30] Z.I. Awal, A study on inland water transport accidents in Bangladesh: experience of a decade (1995-2005), Coast. Ships Inland Waterways 2 (2006), https://doi.org/10.3940/rina.cs.2006.1.
[31] A. Bahramian, M. Mohammadi, G. Ahmadi, Effect of indoor temperature on the velocity fields and airborne transmission of sneeze droplets: an experimental study and transient CFD modeling, Sci. Total Environ. 858 (2023) 159444, https://doi.org/10.1016/j.scitotenv.2022.159444.
[32] T.N. Verma, A.K. Sahu, S.L. Sinha, Study of particle dispersion on one bed hospital using computational fluid dynamics, Mater. Today: Proc. 4 (2017) 10074–10079, https://doi.org/10.1016/j.matpr.2017.06.323.
[33] J. Wang, L. Sun, M. Zou, W. Gao, C. Liu, L. Shang, Z. Gu, Y. Zhao, Bioinspired shape-memory graphene film with tunable wettability, Sci. Adv. 3 (2017), https://doi.org/10.1126/sciadv.1700004.
[34] J.J. Quiñones, A. Doosttalab, S. Sokolowski, R.M. Voyles, V. Castaño, L.T. Zhang, L. Castillo, Prediction of respiratory droplets evolution for safer academic facilities planning amid covid-19 and future pandemics: a numerical approach, J. Build. Eng. 54 (2022) 104593, https://doi.org/10.1016/j.jobe.2022.104593.
[35] J.M. Gwaltney, P.B. Moskalski, J.O. Hendley, Hand-to-hand transmission of rhinovirus colds, Ann. Intern. Med. 88 (1978) 463–467, https://doi.org/10.7326/0003-4819-88-4-463.
[36] J. Howard, A. Huang, Z. Li, Z. Tufekci, V. Zdimal, H.M. van der Westhuizen, A. von Delft, A. Price, L. Fridman, L.H. Tang, V. Tang, G.L. Watson, C.E. Bax, R. Shaikh, F. Questier, D. Hernandez, L.F. Chu, C.M. Ramirez, A.W. Rimoin, An evidence review of face masks against COVID-19, Proc. Natl. Acad. Sci. U.S.A. (2021) 118, https://doi.org/10.1073/pnas.2014564118.